5th International Conference on Durability of Concrete Structures
Jun 30–Jul 1, 2016
Shenzhen University, Shenzhen, Guangdong Province, P.R.China

Edge Detection of Concrete Mesostructure Based on DIS Operator

Bin Feng, Zicheng Xu, Jin Xia, Shijie Jin, and Weiliang Jin
Institute of Structural Engineering, Zhejiang University, Hangzhou, China

ABSTRACT

Aggregate edge detection is the basis of creating concrete mesoscale model, which is applied to analyze concrete mesoscale characteristics. A concrete digital image edge detection method using DIS operator is presented in this paper. Mean filter, multi-scale filter, and Gaussian filter are compared on the effect of concrete image noise reduction. Based on the result, Gaussian filter is the most optimum method to reduce image noise and remain aggregate edge distinct. Sobel operator, Laplacian operator, and DIS operator are applied respectively to detect the aggregate edge on Gaussian filter processed images. Based on the experiment, DIS operator outperforms other two operators in the veracity and integrity of edge detection. It is concluded that using Gaussian filter and DIS operator for edge segmentation can provide geometrical models for FEM analysis.

Keywords: concrete, digital image, Gaussian filter, DIS operator, edge detection, aggregate segmentation

1. INTRODUCTION

Concrete is a typical heterogeneous material composed of aggregate, mortar, interface, and void. Assuming concrete mesoscale model as a mixture of aggregate and mortar with different physical and chemical characteristics can avoid problems in a homogeneity model. Therefore, using concrete mesoscale model to analyze concrete macroscale characteristics is more comparable to actual situation. Concrete macroscale characteristics can be inverted from its inner mechanism.

Aggregate random distribution simulation is the premise and basis for analyzing concrete mesoscale characteristics. During the past decades, researchers mainly present two approaches to create concrete geometrical model. One approach is using algorithm to create simplified aggregate geometry shapes as circles and polygons. In this field, an aggregate distribution method based on 2D circles and 3D spheres was presented (Li, Ma, Chen, & Xu, 2006; Wriggers & Moftah, 2006; Zheng, Li, & Jones, 2003; Zheng, Zhou, & Liu, 2003); by means of aggregate computational random generation, a distribution method using circle, ellipse, and polygon aggregates according to a preset grading curve was presented (Gao, Guan, & Gu, 2006; Li, Xia, & Lin, 2012; Stefan, Stefan, Torsten, & Carsten, 2006; Wang, Kwan, & Chan, 1999; Zhou & Hao, 2009); a method of creating convex polygon was presented in two-dimensional aggregate research (Gao & Liu, 2003; Yin, Yang, Yang, & Jiang, 2011); a method of using 3D spheres and ellipsoids to create concrete geometrical model was realized (Abyaneh, Wong, & Buenfeld, 2013; Du & Sun, 2006); and two-dimensional and three-dimensional random shape aggregates creation was realized based on origin aggregate random prolongation which can be applied in low concentration aggregate concrete (Tehrani, Absi, Allou, & Petit, 2013). This approach which has been wildly used for its high simulation efficiency encounter errors between numerical simulation results and actual test results attribute to the differences in simplified aggregate geometry shape and real aggregate edge.

Another approach is obtaining concrete mesostructure model based on image edge detection, which can more thoroughly reflect aggregate geometrical effect on concrete characteristics. In this field, an edge detection method of computed tomography (CT) image was presented using greyscale threshold conversion, filtration system, etc. (Jiang, Bai, & Peng, 2008; Yang & Buenfeld, 2001; Zhao, Li, Dang, & Chen, 2012); edge detected images obtained by digital image processing technique enabled to measure aggregate physical characteristics directly (Mora, Kwan, & Chan, 1998); Laplacian operator, Canny operator and Roberts operator were separately applied on CT image edge detection (Jiang, Bai, Qi, & Wang, 2008); finite element method and Canny operator were used on digital image edge detection (Qin, Du, & Sun, 2011; Yue, Chen, & Tham, 2003).

Compared with the digital image as shown in Figure 1(b), a CT image has a clearer grayscale threshold, which can accurately separate aggregate from mortar (Duan, Zhang, Li, Wang, & Liu, 2011). Hence, CT images are often used in the second approach of

creating concrete geometrical model. However, CT image edge detection can hardly be applied into large size concrete specimen due to its high technique requirement and high usage cost. Concrete digital image instead requires low cost and is convenient to obtain. Difficulty is its high image noise that often blurs the boundary between aggregate and mortar, which make edge detection method used in CT image improper. Hence, a new noise reduction and edge detection method are requisite for processing concrete digital image. After comparing three noise reduction methods and three detection operators, this paper presents an edge detection method based on Gaussian filter and DIS operator. This method can help build new real aggregate-based geometrical models for concrete mesoscale numerical simulation.

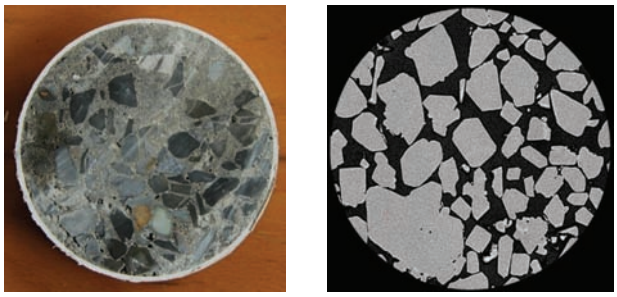

(a) CT image (b) Digital image

Figure 1. Concrete CT image and digital image.

2. CONCRETE SAMPLE DESIGN

2.1 Preparation of concrete sample

Edge detection using DIS operator is based on digital images. For the purpose of verifying advantages and disadvantages between different edge detection algorithms, eight sets of concrete samples are casted. Every set contains five pieces of specimen. The mix design refers to THE DESIGN REGULATIONS OF MIX RATIO OF ORDINARY CONCRETE (JGJ55-2011) and is determined according to the purpose of tests. The 42.5 ordinary Portland cement, 10-mm maximum grain size gravel, and river sand are used to cast concrete. Considering the variation between coarse aggregate, eight sets of samples are designed under the sand ratio as 30, 40, 60, 70, 80, 90, and 100%, as shown in Table 1.

Concrete curing and incision are conducted before obtaining digital images. The ϕ100 mm ± 5 mm × 300 mm round PVC tubes are used as casting molds. After casting, concrete is cured in standard curing chamber (20°C, 95% humidity) for 28 days. When curing process is completed, both ends of concrete are cut for 25 mm and the middle part is divided into five pieces of ϕ100 mm × 50 mm ± 2 mm cylinder. Eight sets of concrete are cut following the same procedure. When cutting process is accomplished, concrete samples are water washed and dried in arid area.

Table 1. Specimen mix design.

	Water/ cement	Cement (kg/m³)	Sand (kg/m³)	Aggregate (kg/m³)	Water (kg/m³)	Sand ratio (%)
S30	0.44	364	551	1285	164	30.00
S40	0.44	364	734	1102	164	40.00
S50	0.44	364	918	918	164	50.00
S60	0.44	364	1102	734	164	60.00
S70	0.44	364	1285	551	164	70.00
S80	0.44	364	1469	367	164	80.00
S90	0.44	364	1642	194	164	90.00
S100	0.44	364	1836	0	164	100.00

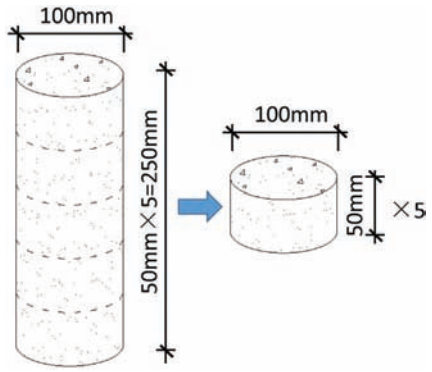

Figure 2. Specimen size.

2.2 Concrete digital image

Concrete samples are photographed under white background successively according to the sand ratio. Canon D60 and EFS18-200mm are used to obtain images. Typical digital images with different sand ratio are shown in Figure 3. Detailed image parameters are listed in Table 2.

Table 2. Digital image parameters.

	Aperture	Exposure time (s)	Focal length (mm)	ISO speed
S30	4.5	1/50	50	100
S40	4.5	1/40	50	100
S50	4.5	1/50	50	100
S60	4.5	1/60	40	100
S70	4.5	1/30	50	100
S80	5.0	1/30	50	100
S90	4.5	1/30	50	100
S100	4.5	1/30	50	100

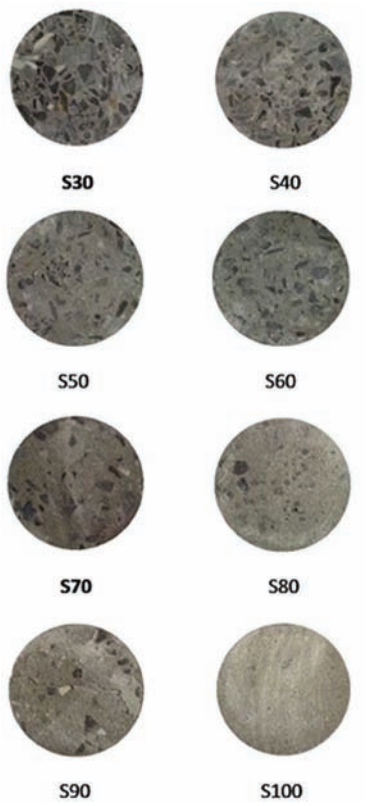

Figure 3. Cut concrete specimen.

3. AGGREGATE EDGE DETECTION

The objective of this paper is using algorithm to automatically segment aggregate from mortar based on grayscale. The aggregate edge detection involves three stages. The first stage is comparing multi-scale filter, mean filter, and Gaussian filter on the effect of concrete image noise reduction and determining the filter applied on concrete digital images. The second stage is comparing Sobel operator, Laplacian operator, and DIS operator on the veracity and integrity of the edge detection results and obtaining aggregate edge pixels. The third stage is filtering obtained pixels, smoothing created aggregate geometry edges, and building geometrical models based on real aggregates for further FEM analysis.

3.1 Concrete digital image characteristics

It is promising to use greyscale as the criteria for aggregate edge detection as shown in Figure 4. Generally, the most significantly greyscale change is the boundary between aggregate and mortar (He, 2009). However, considering the information loss in the inverting from 3D to 2D and the influence of illumination, some errors occur between the detected edge and real aggregate boundary. It is a long-term objective for researchers in image segmentation field to diminish such errors.

In image detection process, second derivative of the greyscale is too sensitive to noise. Generally, derivatives higher than the second will lose its actual applications. Therefore, first or second derivatives are mostly applied in edge detection based on greyscale (Zhang, Song, & He, 2009):

$$\nabla f(x,y) = [f_x, f_y]^T = \left[\frac{\partial f}{\partial x}, \frac{\partial f}{\partial y}\right]^T$$
$$\nabla^2 f(x,y) = \frac{\partial^2 f}{\partial x^2} + \frac{\partial^2 f}{\partial y^2} \quad (1)$$

where f represents the greyscale of concrete digital image; x and y represent greyscale direction.

This paper uses DIS operator based on both first derivative and second derivative of the greyscale. Commonly, the greyscale changes smoothly in concrete digital image. Using first derivative can only obtain incomplete aggregate edge; using second derivative is normally based on zero-cross detection, which can only acquire a few edge pixels (Duan, Li, & Li, 2005). In this paper, the first derivative is used to firstly segment digital images, and second derivative is used in the following for information supplement (Davis, 1975). To further reduce noise influence on the second derivative, noise filter is adopted on digital images.

3.2 Image noise reduction

Gaussian filter is more appropriate for noise reduction in concrete digital images compared with multi-scale filer and mean filter. Illumination changes, image digitalized

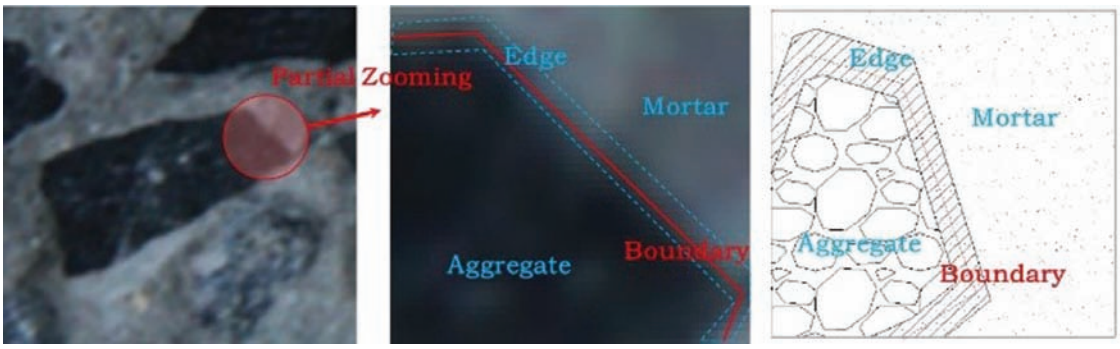

Figure 4. Aggregate edge.

process, and concrete density variations are main source of image noise, which have to be reduced beforehand of edge detection on digital images. According to the actual effect of noise reduction: between multi-scale filter and Gaussian filter, the former caused more edge blur and displacement; between mean filter and Gaussian filter, the effect of noise reduction for concrete digital images is limited using the former one. Hence, Gaussian filter can successfully decline normal distributed noise for digital images (Deng & Cahill, 1993). It recalculates the value of every pixel by taking a weighted average of its greyscale and the surround pixels' greyscale. The coefficient of the weighted average is obtained and normalized using a two-dimensional discrete Gaussian function (Wang, 2010):

$$f(x,y) = \frac{1}{2\pi\sigma^2} e^{\frac{-(x^2+y^2)}{2\sigma^2}} \quad (2)$$

where f represents greyscale of the concrete digital image; x and y represent greyscale direction.

An original image and a Gaussian filter processed image are shown in Figures 5(a) and (b). The filtered image has been smoothed attributable to noise reduction.

(a) Original image (b) Noise reduced image

Figure 5. Gaussian filter processed image.

3.3 Edge detection operator

3.3.1 DIS operator

DIS (difference in strength) operator has been broadly used in image segmentation area. On inputted concrete digital images, a 3×3 pixel window as shown in Figure 6 is used to separately calculate every pixel's DIS value according to function (3).

$$\begin{aligned} &|f_1 - f_3| + |f_1 - f_5| + |f_1 - f_6| + |f_1 - f_7| + \\ &|f_1 - f_8| + |f_2 - f_4| + |f_2 - f_5| + |f_2 - f_6| + \\ &|f_2 - f_7| + |f_2 - f_8| + |f_3 - f_4| + |f_3 - f_6| + \\ &|f_3 - f_7| + |f_3 - f_8| + |f_4 - f_5| + |f_4 - f_7| + \\ &|f_4 - f_8| + |f_5 - f_6| + |f_5 - f_7| + |f_6 - f_8| \end{aligned} \quad (3)$$

where f represents pixel's greyscale value and number represents the pixel position in the pixel window.

Since the pixels' greyscale in aggregate and mortar has an inclination towards different values, aggregate can be segmented from its background by setting a greyscale threshold to filter out pixels inside aggregates as shown in Figure 7. Pixels' greyscale value both inside aggregate and inside mortar changes smoother after image noise have been reduced by Gaussian filter, while the value near aggregate edge changes more dramatically. Hence, pixels obtaining large DIS value have a higher possibility to be the boundary between aggregate and mortar.

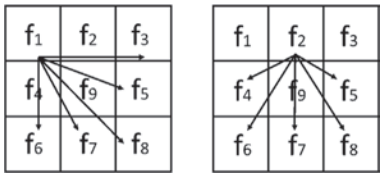

Figure 6. The Pixel window of DIS edge detection.

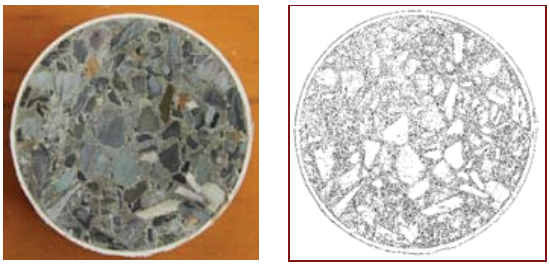

(a) Original image (b) Threshold processed detected image

Figure 7. Aggregate detection using DIS operator.

3.3.2 Edge detection operator comparison

DIS operator has gradually been applied in image segmentation area in recent years. Sobel operator and Laplacian operator have been widely used for decades. These three operators have different mathematic calculation methods and process characteristics as shown in Table 3.

Table 3. Comparison on characteristics of edge detection operators.

Operator	Definition
Sobel	$G_x = \begin{bmatrix} -1 & 0 & +1 \\ -2 & 0 & +2 \\ -1 & 0 & +1 \end{bmatrix} \times A$
	$G_y = \begin{bmatrix} -1 & -1 & -1 \\ 0 & 0 & 0 \\ +1 & +2 & +1 \end{bmatrix} \times A$
Laplacian	$\nabla^2 f = \frac{\partial^2 f}{\partial x^2} + \frac{\partial^2 f}{\partial y^2}$
DIS	$\begin{aligned} &\|f_1 - f_3\| + \|f_1 - f_5\| + \|f_1 - f_6\| + \|f_1 - f_7\| + \|f_1 - f_8\| + \\ &\|f_2 - f_4\| + \|f_2 - f_5\| + \|f_2 - f_6\| + \|f_2 - f_7\| + \|f_2 - f_8\| + \\ &\|f_3 - f_4\| + \|f_3 - f_6\| + \|f_3 - f_7\| + \|f_3 - f_8\| + \|f_4 - f_5\| + \\ &\|f_4 - f_7\| + \|f_4 - f_8\| + \|f_5 - f_6\| + \|f_5 - f_7\| + \|f_6 - f_8\| \end{aligned}$

3.3.3 Noise reduced image

Gaussian filter is applied in concrete digital images to reduce environment noise. Sobel operator, Laplacian operator, and DIS operator are separately applied to detect aggregate edge based on pixels greyscale value as shown in Figure 8.

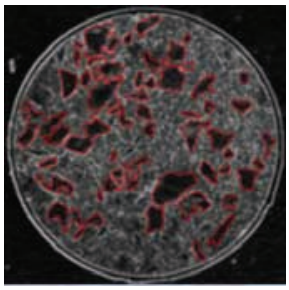

(a) Sobel

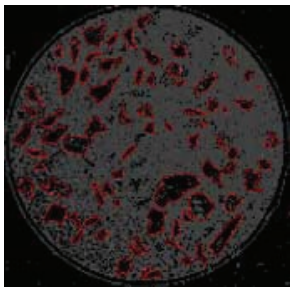

(c) DIS

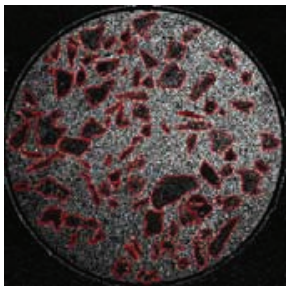

(b) Laplacian

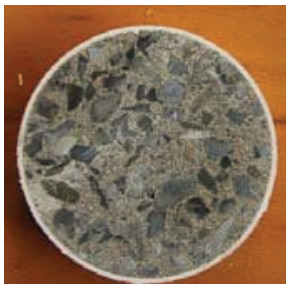

(d) Original

Figure 8. Edge detection of noise reduced images.

Considering concrete digital image characteristics, noise reduced images and noise enhanced images are used for comparing operators edge detection results.

3.3.4 Noise enhanced image

Gaussian noise with zero mean and σ2 standard deviation is applied on digital images. When image environment noise doesn't conform to normal distribution, pixels around abnormal value have a possibility to be determined as edge feature points (Xu, 2007) because Gaussian filter result is aberrant around abnormal value pixels, which means the width of aggregate edge is anomalous. Sobel operator, Laplacian operator and DIS operator have been applied on noise enhanced image as shown in Figure 9.

Comparing the edge detection result, DIS operator performs a higher veracity and integrity than Sobel operator. Images segmented by Sobel operator display a bilateral effect and have a wider edge as shown in Figures 8(a) and (c) due to the loss of boundary information by calculating in a

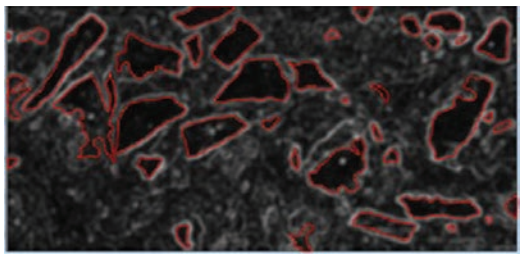

(a) Sobel

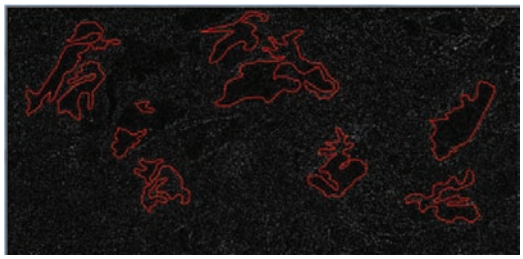

(b) Laplacian

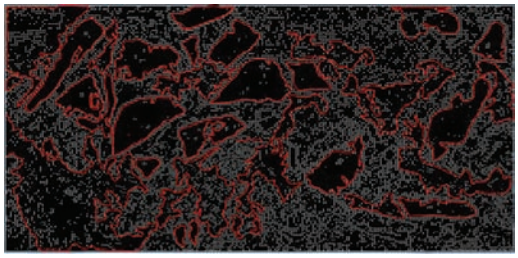

(c) DIS

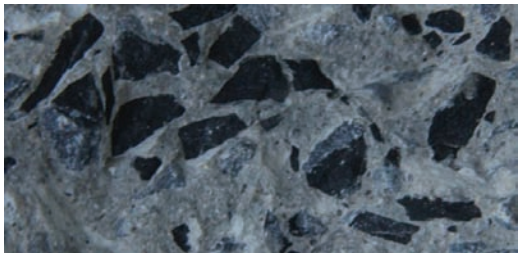

(d) Original

Figure 9. Edge detection of noise enhanced images.

relatively large scale template. The disadvantage distinguishes in noise enhanced environment as shown in Figures 9(a) and (c). Hence, digital images detected by Sobel operator behave a notable bilateral effect under low noise situation and obtain few feature points under high noise situation.

Comparing results of DIS operator and Laplacian operator, the latter is more efficient in determine the side a pixel locates on a digital image (Huang & Zheng, 2008) rather than detect the boundary. Laplacian operator is more sensitive to noise and creates many pseudo edge on images which numerous overlapped

and coiled edges are detected (Sorkine et al., 2004) in non-edge areas as shown in Figures 8(b) and (c). Additionally, it is difficult to reach a balance between veracity and integrity for Laplacian operator as shown in Figure 9(b).

The following edge tracing algorithm is built upon detected pixels. Tracing objects are weak edge pixels that have mapping function values higher than low threshold but lower than high threshold. The numbers of detected edge pixels will mostly determine the finale segmented aggregate edge quality. Hence, DIS operator which has rich edge information and strong anti-noise capacity can improve the integrity and continuity of aggregate edge.

DIS operator using eight neighboring pixel relations can acquire more abundant edge information than Sobel operator and is less sensitive to noise than Laplacian operator. Therefore, DIS operator is more proper to be used in segmenting aggregate edge where image noise is distinct and wild in distribution.

3.4 Edge detection optimization

Optimization on edge detected image is necessary for further usage. According to different aggregate size, hundreds or thousands pixels are detected to describe the geometry shape of one aggregate. Directly linking every pixel can precisely delineate the geometry shape, while computational complexity in further database building and application will increase to an unreasonable level. By calculating the slope changes in every three continuous detected pixels, some pixels having a mild slope change are eliminated, which can effectively reduce computational complexity under the condition of preventing aggregate geometry shape from distortion. The process of linking the remaining pixels, smoothing line segment, and saving aggregate geometry into database are shown in Figure 10.

4. EDGE DETECTION ANALYSIS

The edge detection method presented is applied on all eight sets of concrete digital images. The results of image S40 and S60 are shown in Figure 11. Eight sets of digital images results comparison is presented in Table 4. Comparing detected aggregates area using DIS operator and the actual aggregates area in concrete section, S70 has the most distinct segmentation error. Three reasons of occurring edge detection errors can be concluded: (1) greyscale diversity inside aggregates due to material characteristics and environment affects detection veracity; (2) aggregates distributing sparsely in concrete section causes detection error; and (3) concrete section not being level and remained environment noise influence detection veracity and integrity.

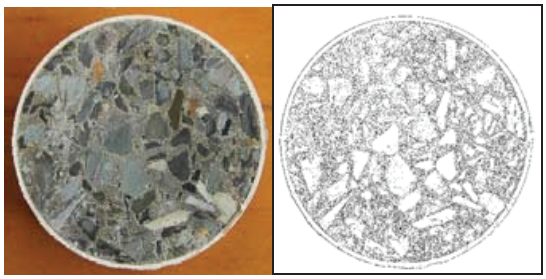

(a) S40

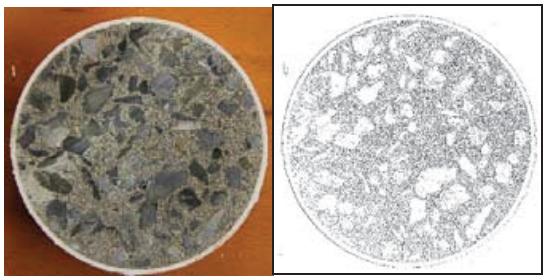

(b) S60

Figure 11. Result of DIS edge detection.

Table 4. Comparison of detected aggregate area.

	Assumed aggregate area ratio (%)	Detected aggregate area ratio (%)	Detected aggregate number	Actual aggregate number
S30	70	63.26	63	70
S40	60	57.48	64	73
S50	50	65.83	61	65
S60	40	35.07	54	56
S70	30	21.73	37	43
S80	20	16.36	13	19
S90	10	15.72	15	21
S100	0	0.39	4	0

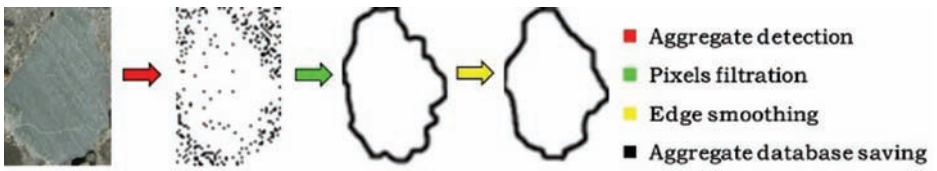

Figure 10. Optimization after edge detected.

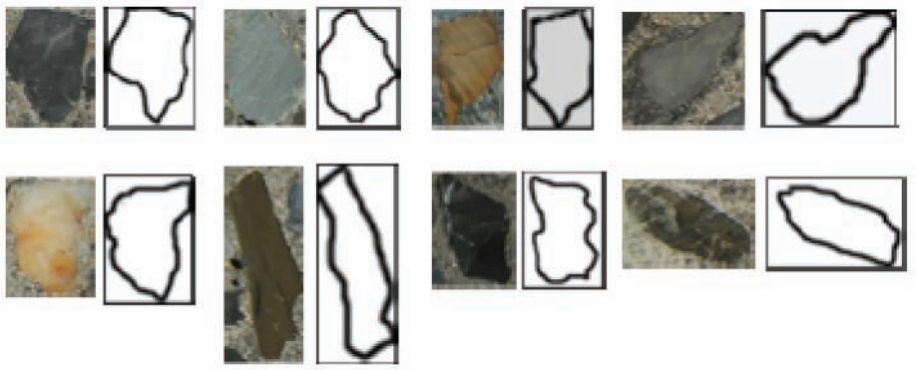

Figure 12. Comparison of real aggregate geology with detected aggregate geology.

In developing aggregate segmentation accuracy, three improvements can be implemented in the future: (1) enhancing greyscale differences between aggregate and mortar; (2) increasing digital image quality; and (3) improving concrete section leveling and reducing errors caused by illumination and shadow.

Comparison between real aggregate shapes and their detected aggregate geometry shapes are shown in Figure 12. The veracity and integrity of detected edge improve in area where the greyscale of real aggregate edge is distinct from the greyscale of surrounding mortar. Diverse greyscales inside aggregate perform an adverse effect on edge detection results.

5. CONCLUSION

This paper presents an edge detection method for concrete digital images using Gaussian filter to reduce image noise and DIS operator to segment aggregate from mortar: (1) from detection results, using Sobel operator to detect concrete digital images will lose many edge information attribute to its relative large calculation template; using Laplacian operator in images will cause segmentation errors due to its sensitivity to image noise; and DIS operator will efficiently obtain integral and accurate aggregate geometrical shapes; (2) from segmentation method, DIS operator replace convolution of directional derivative with eight neighboring pixel relations, which can acquire smooth edge information in low noise environment and obtain relative integral edge information in high noise environment. This method is superior to Sobel operator and Laplacian operator by eliminating adverse effect of choosing greyscale threshold manually; and (3) future development in edge detection of using DIS operator: DIS operator detected results are related to pixel numbers in a digital image; when the greyscale change inside aggregate is relative large and is comparative smooth on the edge, errors occur in DIS detected image.

ACKNOWLEDGMENTS

This work was supported by the Natural Science Foundation of China (51408537), the Key Program from the Natural Science Foundation of Zhejiang Province (LZ16E080002), and the European Union Research Council *via* a research grant (FP7-PEOPLE-2011-IRSES-294955).

REFERENCES

Abyaneh, S. D., Wong, H. S., & Buenfeld, N. R. (2013). Modelling the diffusivity of mortar and concrete using a three-dimensional mesostructure with several aggregate shapes. *Computational Materials Science*, *78*, 63–73.

Davis, L. S. (1975). A survey of edge detection techniques. *Computer Graphics and Image Processing*, *4*(3), 248–270.

Deng, G., & Cahill, L. W. (1993). An adaptive Gaussian filter for noise reduction and edge detection. *IEEE*, 1615–1619.

Du, C. B., & Sun, L. G. (2006). Numerical simulation of concrete aggregates with arbitrary shapes and its application. *Journal of Hydraulic Engineering*, *6*, 003.

Duan, R. L., Li, Q. X., & Li, Y. H. (2005). Summary of image edge detection. *Optical Technique*, *31*(3), 415–419.

Duan, Y. H., Zhang, X. N., Li, Z., Wang, D. Y., & Liu, Y. S. (2011). Methods about digital representation on surface profile of concrete aggregates from 2-D to 3-D based on X-ray computed tomography. *China Journal of Highway and Transport*, *24*(6), 9–15.

Gao, Q., Guan, Z., & Gu, Y. (2006). Automatic generation of finite element model for concrete aggregate. *Journal-Dalian University of Technology*, *46*(5), 641.

Gao, Z. G., & Liu, G. T. (2003). Two-dimensional random aggregate structure for concrete. *Qinghua Daxue Xuebao/Journal of Tsinghua University (China)*, *43*(5), 710–714.

He, J. H. (2009). *Study on microstructure and properties of road cement concrete*. Xi'an, China: Chang'an University.

Huang, J. L., & Zheng, X. M. (2008). Improved image edge detection algorithm based on Canny operator. *Computer Engineering and Application*, *44*(25), 170–172.

Jiang, Y., Bai, W., & Peng, G. (2008). Edge detection of concrete mesostructure with ct image. *Engineering Journal of Wuhan University*, *1*(41), 77–80.

Jiang, Y., Bai, W., Qi, Y. L., & Wang, Q. F. (2008). Reconstruction of 3d model of concrete mesastructure with CT original data. *Journal of China Three Gorges University (Natural Sciences)*, *1*, 014.

Li, L. Y., Xia, J., & Lin, S. S. (2012). A multi-phase model for predicting the effective diffusion coefficient of chlorides in concrete. *Construction and Building Materials*, *26*(1), 295–301.

Li, Y. C., Ma, H. F., Chen, H. Q., & Xu, X. (2006). Approach to generation of random convex polyhedral aggregate model and plotting for concrete meso-mechanics. *Journal of Hydraulic Engineering*, *5*, 588–592.

Mora, C. F., Kwan, A. K. H., & Chan, H. C. (1998). Particle size distribution analysis of coarse aggregate using digital image processing. *Cement and Concrete Research*, *28*(6), 921–932.

Qin, W., Du, C. B., & Sun, L. G. (2011). Meso-level analysis model for concrete based on digital image processing. *Journal of Hydraulic Engineering*, *4*, 011.

Sorkine, O., Cohen-Or, D., Lipman, Y., Alexa, M., Rossl, C., & Seidel, H. (2004). Laplacian surface editing. *ACM*, 175–184.

Stefan, H., Stefan, E., Torsten, L., & Carsten, K. (2006). Mesoscale modeling of concrete: Geometry and numerics. *Computers & Structures*, *84*(7), 450–461.

Tehrani, F. F., Absi, J., Allou, F., & Petit, C. (2013). Heterogeneous numerical modeling of asphalt concrete through use of a biphasic approach: Porous matrix/inclusions. *Computational Materials Science*, *69*, 186–196.

Wang, D. (2010). *Image edge detection method based on anisotropic Gaussian filtering*. Xi'an, China: Xidian University.

Wang, Z. M., Kwan, A. K. H., & Chan, H. C. (1999). Mesoscopic study of concrete I: Generation of random aggregate structure and finite element mesh. *Computers & Structures*, *70*(5), 533–544.

Wriggers, P., & Moftah, S. O. (2006). Mesoscale models for concrete: Homogenisation and damage behaviour. *Finite Elements in Analysis and Design*, *42*(7), 623–636.

Xu, J. B. (2007). *Study on approximation theory and application of Gaussian filter*. Heilongjiang, China: Harbin Institute of Technology, pp. 14–74.

Yang, R., & Buenfeld, N. R. (2001). Binary segmentation of aggregate in SEM image analysis of concrete. *Cement and Concrete Research*, *31*(3), 437–441.

Yin, A. Y., Yang, X. H., Yang, S. F., & Jiang, W. (2011). Multiscale fracture simulation of three-point bending asphalt mixture beam considering material heterogeneity. *Engineering Fracture Mechanics*, *78*(12), 2414–2428.

Yue, Z. Q., Chen, S., & Tham, L. G. (2003). Finite element modeling of geomaterials using digital image processing. *Computers and Geotechnics*, *30*(5), 375–397.

Zhang, B., Song, Y., & He, A. (2009). Edge detection based on derivative algorithm in arbitrary directions. *Opto-Electronic Engineering*, *10*, 027.

Zhao, L., Li, C. H., Dang, F. N., & Chen, D. F. (2012). Architecture concrete mesostructure analysis based on CT image fracture process. *Advanced Materials Research*, *368-373*, 2638–2641.

Zheng, J. J., Li, C. Q., & Jones, M. R. (2003). Aggregate distribution in concrete with wall effect. *Magazine of Concrete Research*, *55*(3), 257–265.

Zheng, J. J., Zhou, X. Z., & Liu, Y. Q. (2003). Simulation of 2-d distribution of concrete aggregates and its application. *Journal of Hydraulic Engineering*, *7*, 80–85.

Zhou, X. Q., & Hao, H. (2009). Mesoscale modelling and analysis of damage and fragmentation of concrete slab under contact detonation. *International Journal of Impact Engineering*, *36*(12), 1315–1326.